

Structure and biosynthetic implication of (*S*)-NHAB, a novel shunt product, from a disruptant of the *actVI*-ORFA gene for actinorhodin biosynthesis in *Streptomyces coelicolor* A3(2)

Makoto Ozawa,^a Takaaki Taguchi,^a Takayuki Itoh,^a Yutaka Ebizuka,^a Kevin I. Booker-Milburn,^b G. Richard Stephenson^c and Koji Ichinose^{a,*}

^aGraduate School of Pharmaceutical Sciences, The University of Tokyo, Hongo, Bunkyo-ku, Tokyo 113-0033, Japan

^bSchool of Chemistry, University of Bristol, Cantock's Close, Bristol BS8 1TS, UK

^cWolfson Materials and Catalysis Centre, School of Chemical Sciences and Pharmacy, University of East Anglia, Norwich NR4 7TJ, UK

Received 24 July 2003; accepted 8 September 2003

Abstract—A novel shunt product was isolated from a disruptant of the *actVI*-ORFA gene involved in the biosynthesis of actinorhodin (ACT) in *Streptomyces coelicolor* A3(2). Its structure was elucidated as 1,4-naphthoquinone-8-hydroxy-3-[3(*S*)-acetoxy-butyrac acid], (*S*)-NHAB, based on NMR, MS, and CD spectroscopic data as well as a single crystal X-ray crystallographic analysis. The formation of (*S*)-NHAB involves a retro-Claisen type C–C bond cleavage of an ACT biosynthetic intermediate. Feeding experiments with [¹⁻¹³C] and [2-¹³C] acetates indicated its biosynthetic origin as a single octaketide chain. The relevant gene product, Act-ORFA, which is a functionally unknown protein, is proposed to play a regulatory role related to the multi-enzymatic steps to ACT production, based on the metabolic profile of its disruptant and the wide distribution of *actVI*-ORFA homologues in the gene clusters for *Streptomyces* aromatic polyketides.
© 2003 Elsevier Ltd. All rights reserved.

1. Introduction

S. coelicolor A3(2) is the most genetically characterized streptomycete, with a complete genome sequence,¹ producing at least four metabolically distinct antibiotics, allowing for studies on antibiotic biosynthesis as well as on their metabolic relationships with primary metabolism and morphological differentiation.² One of the antibiotics, actinorhodin (ACT, **1**),³ belongs to a class of *Streptomyces* aromatic antibiotics known as benzoisochromanquinones (BIQs) (Chart 1). Biosynthetic studies on the BIQs provide a number of interesting problems concerning the formation of a fundamental polyketide skeleton by a type II polyketide synthase (PKS)⁴ followed by post-PKS modification ('tailoring') steps.⁵ Earlier genetic and biochemical studies revealed⁴ the ACT biosynthetic gene cluster (the *act* cluster) spanning over 22 kb with 22 open reading frames (ORFs). We are particularly interested in the BIQ tailoring steps,⁵ including stereochemical control,⁶ oxygenation,⁷ and modification via C–C bond formation either by glycosylation^{8,9} (granaticin, GRA, **2** and medermycin, MED, **3**) or by dimerization¹⁰ (ACT). The *actVI* genetic region¹¹ (ORFA, 1, 2, 3, 4), part of the *act* cluster, is largely related to

stereospecific pyran ring formation. Our previous chemical characterization^{12,13} of disruptants of the *actVI* region revealed that disruption of ORFA led not only to significant reduction in ACT production, but also to production of an unknown compound X, together with the known intermediate, 4,10-dihydro-9-hydroxy-1-methyl-10-oxo-3*H*-naphtho[2,3-*c*]pyran-3-(*S*)-acetic acid, (*S*)-DNPA (**4**) (Chart 1).^{14,15} We describe here its structure elucidation and origin in relation to ACT biosynthesis.¹⁶

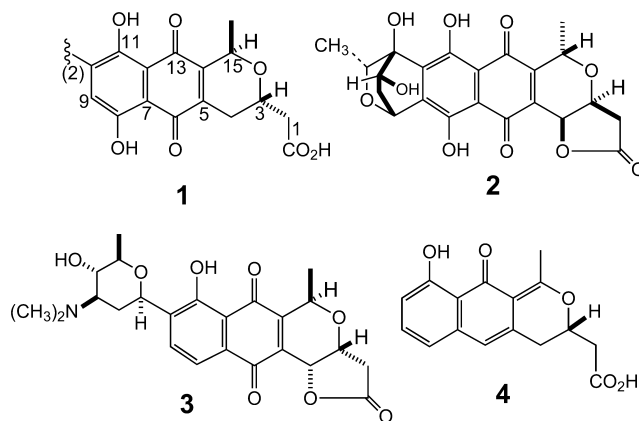


Chart 1. Structures of the BIQ antibiotics and related metabolites: actinorhodin (**1**); granaticin (**2**); medermycin (**3**); (*S*)-DNPA (**4**).

Keywords: aromatic polyketides; actinorhodin; biosynthesis; *Streptomyces*.

* Corresponding author. Tel.: +81-3-5841-4742; fax: +81-3-5841-4744; e-mail: ichinose@mol.f.u-tokyo.ac.jp

Table 1. NMR data for **5** (in CDCl₃, 500 MHz for ¹H; 125 MHz for ¹³C)

Position	¹³ C		¹ H			Carbon(s) correlated in HMBC spectrum
	δ (ppm)	δ (ppm)	Intensity	Multiplicity	<i>J</i> (Hz)	
1	174.1					
2	38.5	2.74 ^a	2H	d d-like ^a	<i>J</i> =6.0, 7.0	C-1, 3, 4
3	68.4	5.47	1H	m		
4	34.3	2.78	1H	d d d	<i>J</i> =14.0, 8.5, 1.0	C-2, 3, 5, 6, 14
		3.07	1H	d d d	<i>J</i> =14.0, 4.5, 1.0	C-2, 3, 5, 6, 14
5	147.9					
6	183.9					
7	131.9					
8	119.6	7.66	1H	d d	<i>J</i> =8.0, 1.5	C-6, 10, 12
9	136.4	7.62	1H	t	<i>J</i> =8.0	C-7, 11
10	124.4	7.27	1H	d d	<i>J</i> =8.0, 1.5	C-8, 12
11	161.4	11.87	1H (OH)	s		C-10, 11, 12
12	115.1					
13	187.8					
14	136.8	6.81	1H	s		C-4, 6, 12
15	170.2					
16	20.8	2.01	3H	s		C-15

^a The band centre for two overlapping signals, and *J* values are uncorrected for second order effects.

2. Results and discussion

2.1. Isolation and structure elucidation

Our earlier chemical characterization based on HPLC analysis showed¹³ that compound X has a UV–VIS spectrum similar to that of **4**, with a characteristic absorbance maximum in the visible region (410 nm). The production medium from a large-scale culture of the *actVI*-ORFA disruptant was extracted with chloroform. The residue from the concentrated extracts was subjected to repeated silica-gel column chromatography in chloroform–ethyl acetate to purify compound X, which was used for extensive spectroscopic studies.

High-resolution EI–MS measurement indicated its molecular formula to be C₁₆H₁₄O₇ (found: 318.0785; requires 318.0740). The major fragment peaks, besides the molecular ion peak (*m/z* 318), in the EI–MS spectrum were *m/z* 214 (base peak) and *m/z* 258. The ¹H NMR and ¹³C NMR spectra showed similar signal patterns to those of **4**, suggesting the presence of fused bicyclic A–B rings. The characteristic ¹H NMR signal for a terminal methyl signal of C-16 at 2.01 ppm is shifted to upper-field by ca. 0.6 ppm from that of **4**, indicating that a major structural difference is present involving C-15. Further extensive 2D NMR measurements using HMQC and HMBC unambiguously established full assignments of the signals of ¹H NMR and ¹³C NMR spectra and their key correlations (Table 1). The C–C bond between C-14 and C-15 is disconnected to provide an acetoxy moiety derived from C-15 and C-16, thus explaining the shift of the methyl ¹H NMR signal mentioned above. The proposed structure is in perfect agreement with the fragmentation peaks of the EI–MS: the elimination of the acetoxy moiety at C-3 and decarboxylation at C-1 give the naphthoquinone fragment at *m/z* 214; the remaining fragments also clearly reflect the elucidated structure, 1,4-naphthoquinone-8-hydroxy-3-[3-acetoxybutyric acid], NHAB.

The CD spectrum of **4** shows a distinct positive Cotton

effect centred at around 435 and 330 nm,^{6,14} which is apparently attributed to a conjugated tricyclic system. The C-3 epimer of **4**, (*R*)-DNPA, gives a CD curve with the mirror image of that of **4**,⁶ indicating the unique C-3 stereogenic centre to be a determinant of the chirality sign. The CD (Fig. 1) of X showed a weak positive Cotton effect at the same wavelength (435 and 330 nm), assignable to the naphthoquinone chromophore of X. Although the consistency of the CD patterns of **4** and X is not simply indicative of their same stereochemistry at C-3, there is a possibility that the Cotton effect would be applicable to the aromatic chirality method¹⁷ to determine the C-3 absolute stereochemistry using the benzoate derivative of X. The molecular structure was also confirmed by a single crystal X-ray crystallographic analysis (Fig. 2). All of the combined analytical data together with the assumption of the biosynthetic relationship with ACT elucidated X to be (*S*)-NHAB (**5**) (Chart 2).

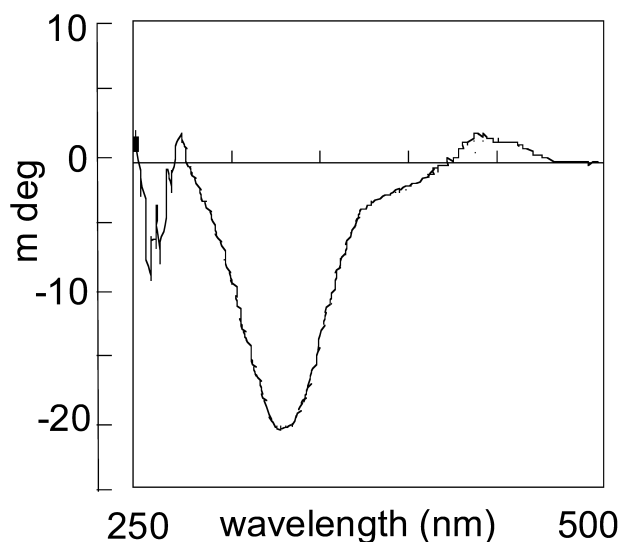


Figure 1. CD spectrum of **5**.

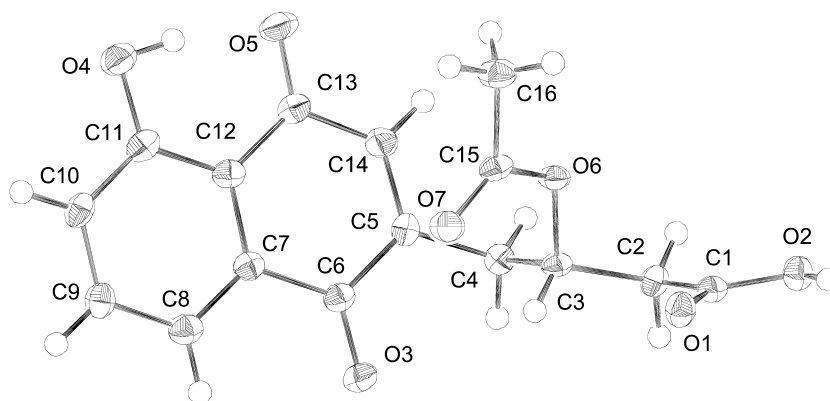


Figure 2. ORTEP view of **5**, showing ellipsoids at 50% probability level.

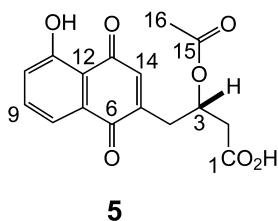


Chart 2. Structure of (*S*)-NHAB (**5**).

2.2. Biosynthetic study using labelled acetates

^{13}C -Labelling experiments were carried out to clarify the biosynthetic origin of underlying carbon skeleton of **5**. Highly specific incorporation of label at the expected positions (C-1, 3, 5, 7, 9, 11, 13, and 15 from $[1-^{13}\text{C}]$ acetate, Fig. 3b; C-2, 4, 6, 8, 10, 12, 14, and 16 from $[2-^{13}\text{C}]$ acetate, Fig. 3a) at comparable levels, indicated its origin as a single polyketide chain. Further supporting evidence was obtained from a feeding experiment using $[2-^{13}\text{C}, ^2\text{H}_3]$ acetate without intact incorporation of an acetate unit into the terminal acetoxy moiety of **5** (see Section 3). This agrees

with the fact that acetyl-CoA is not used directly as a starter unit, which is provided by decarboxylation of malonyl-ACP, in ACT biosynthesis.¹⁸ Similarly, no intact incorporation of acetate into the terminal position was observed for the biosynthesis of the aromatic polyketide antibiotic, tetracenomycin C, in *Streptomyces glaucescens*.¹⁹

2.3. Biosynthetic implication

The middle biosynthetic steps of **1** involve the formation of hemiketal **7a** derived from the secondary alcohol **6** followed by dehydration to afford **4** (Fig. 4).^{12,13} Interruption of this stepwise mechanism would allow an isomerisation of **7a** to **7b** followed by cleavage of the C–C bond between C-14 and C-15 to afford the dihydroxynaphthalene **8**, which could biosynthetically tautomerize to a seminaphthoquinone form susceptible to (spontaneous) oxidation to **5**. Mechanistically, the C–C bond cleavage at C-14 and C-15 is regarded as a retro-Claisen type reaction. A similar mechanistic proposal was made for the simultaneous production of the BIQ antibiotics and juglomycins (Chart 3) by *Streptomyces* strains.²⁰ Hydrolysis of the acetyl moiety of **8** followed by

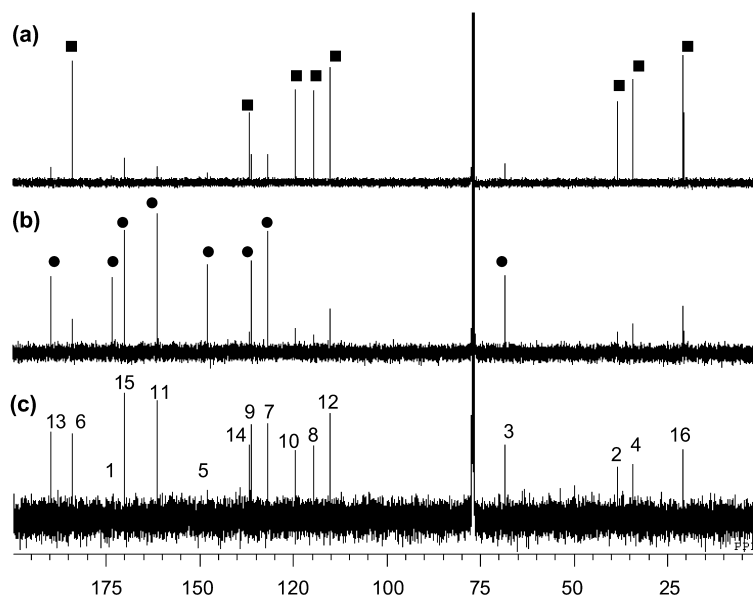


Figure 3. ^{13}C NMR spectra of **5**: (a) labelled with $[2-^{13}\text{C}]$ acetate; (b) labelled with $[1-^{13}\text{C}]$ acetate; (c) non-labelled. Enriched positions are indicated with either filled circles or squares.

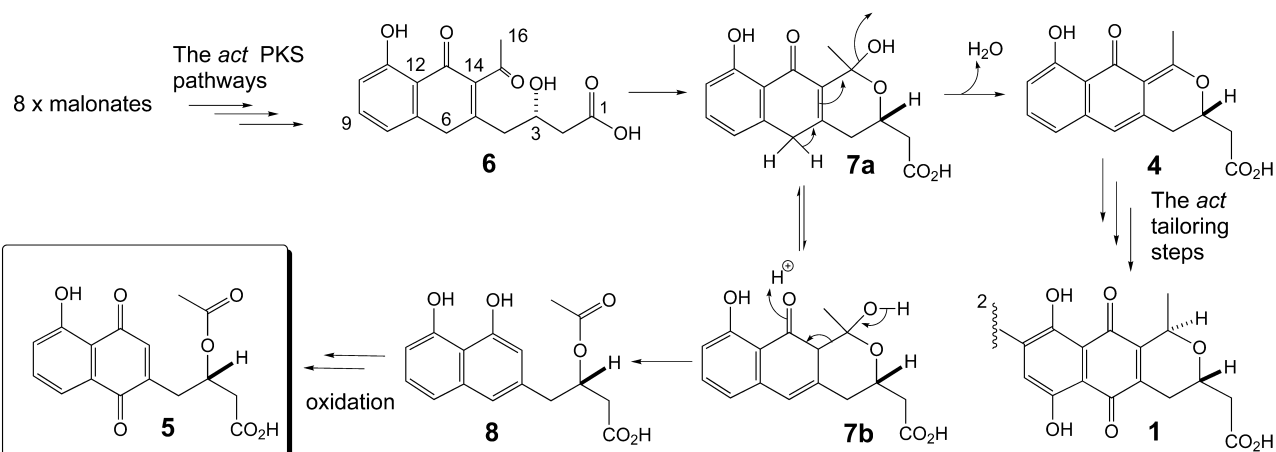


Figure 4. Proposed biosynthetic pathway of actinorhodin (1) and shunt pathway leading to 5.

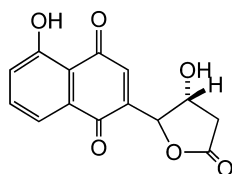


Chart 3. Structure of juglomycin A.

oxidation and lactonisation would lead to a juglomycin-type intermediate. Our present study provided a clear demonstration of a retro-Claisen type metabolic reaction by genetic manipulation.

Disruption of *actVI-ORFA* caused accumulation of the intermediate 4 as well as the shunt product 5 without complete abolition of ACT production. One could deduce that the ORFA product might function as a cyclase or dehydratase to assist the chemically spontaneous formation of 7a and its dehydration for efficient pyran ring formation. However, database search for the *actVI-ORFA* homologues revealed a family of genes widely found in the gene clusters for *Streptomyces* aromatic polyketides, not restricted to the BIQs, but also related to compounds exclusively with carbocyclic ring systems. They include *fren-ORFX* from the putative frenolicin cluster of *S. roseofulvus*,²¹ *gra-ORF31* from the GRA cluster of *Streptomyces violaceoruber* Tü22,⁸ *med-ORF10* from the MED cluster of *Streptomyces* sp. AM-7161,⁹ *mtmX* from *Streptomyces argillaceus*,²² *dpsH* from the daunorubicin clusters of *Streptomyces peuceetius*,^{23,24} and *Streptomyces* sp. strain C5.²⁵ Functional analysis of *dpsH* was made by its heterologous co-expression with type II PKS genes, resulting in favourable production of the tricyclic aklanonic acid instead of a monocyclic shunt product.²³ A plausible role of DpsH as a cyclase was not confirmed by the later mutational study,²⁴ where a *dpsH* disruptant mainly accumulated a tetracyclic intermediate, ϵ -rhodomycinone. Although no definite role can be deduced from the available data, the products of the *actVI-ORFA* family of genes certainly play a crucial role in the efficient production of aromatic polyketides. We proposed¹⁶ a more general role of the gene products concerning the stability of the multicomponent, type II PKS complex, and closely related post-PKS tailoring enzymes. Comparative studies on

the expression levels of the key biosynthetic enzymes in ACT biosynthesis in mutant and wild type are in progress.

3. Experimental

3.1. General

Melting points were determined on a Yanagimoto micro melting point apparatus and uncorrected. Column chromatography was carried out with Wakogel C-200 impregnated with oxalic acid. TLC was conducted on a 0.25 mm precoated silica gel plate (60F₂₅₄, Merck). NMR spectra were recorded on a JEOL Alpha-500 spectrometer (500 MHz for ¹H; 125 MHz for ¹³C; 77 MHz for ²H) in chloroform-*d* with TMS as a reference. Chemical shifts are expressed as δ in ppm. Mass spectra were recorded on a JEOL MStation JMS-700 spectrometer. Optical rotation was determined on a JASCO P-1010 digital polarimeter. CD spectrum was measured on a stopped flow circular dichroism spectrometer model 202SF (AVIV[®] Instruments Inc.).

3.2. Chemicals

Sodium [1-¹³C] acetate (99 atom% ¹³C), sodium [2-¹³C] acetate (99 atom% ¹³C), sodium [2-¹³C, ²H₃] acetate (99 atom% ¹³C and ²H) were purchased from Isotec Co., Ltd, and MSD Isotopes Co., Ltd.

3.3. Bacterial strains and culture conditions

S. coelicolor A3(2) J1501²⁶ (*hisA1 uraA1 strA1 pgl SCP1⁻ SCP2⁻*) was an original actinorhodin-producing strain. The gene disruptant of *actVI-ORFA* in J1501 was as described previously.¹¹ Standard growth conditions for *Streptomyces* strains and disruptants were as follows.²⁷ Seed cultures (10 mL) were grown in 50 mL culture tubes containing glucose 2%, peptone (DIFCO) 0.3%, beef extract (DIFCO) 0.3%, yeast extract (DIFCO) 0.1%, NaCl 0.3%, CaCO₃ 0.1%, pH 7.0, on a rotary shaker (220 rpm) at 30°C for 2 days. Aliquots of the culture were transferred to 50 mL of production medium (pH 7.0) consisting of glycerol 1.5%, soybean meal (Nissin Soya Flour F-T) 1%, and NaCl 0.3%

in 500 mL Erlenmeyer flasks which were grown shaking (200 rpm) at 28°C for 4 days.

3.4. Isolation and purification of (S)-NHAB (5)

The production medium from a large-scale culture (5.1 L) of the *actVI*-ORFA disruptant was extracted with chloroform. The residue from the concentrated extracts was subjected to repeated column chromatography on oxalic acid-impregnated silica gel in chloroform-ethyl acetate to purify (S)-NHAB (5) (11 mg). A single crystal (yellow block, mp 172°C) was obtained from methanol for X-ray crystallographic analysis.

3.5. Optical rotation and CD spectrum

$[\alpha]_D = -82.4$ ($c=0.05$, CHCl_3). CD measurement was performed at the concentration of 1.4 g/L in acetonitrile at 25°C: sampling every 1.0 nm; averaging time, 5.00 s. θ_{max} (m deg): 435 (1.90), 330 (−20.89).

3.6. X-Ray crystallographic study

A crystal of 5 having approximate dimensions of 0.25×0.15×0.10 mm³ was used. All measurements were made on a Rigaku RAXIS RAPID Imaging Plate diffractometer with graphite-monochromated Mo K α radiation at 103 K to a maximum 2θ value of 60.1°. Of the 16856 collected reflections, 4156 were unique ($R_{\text{int}}=0.057$): C₁₆H₁₄O₇, MW=318.28, triclinic, space group $P1(\#1)$, $a=7.167(2)$ Å, $b=10.251(3)$ Å, $c=11.052(3)$ Å, $\alpha=116.00(3)^\circ$, $\beta=90.16(2)^\circ$, $\gamma=91.80(3)^\circ$, $V=729.3(4)$ Å³, $Z=2$, $D_{\text{calc}}=1.449$ g cm^{−3}, $F_{000}=332.00$, $\mu=1.115$ cm^{−1}. The structure was solved by direct methods (SHELXS-97)²⁸ and refined by full-matrix least-squares techniques performed to minimize $\sum w(F_o^2 - F_c^2)^2$ (CRYSTALS).²⁹ The final $R1$, Rw and goodness of fit indicator were 0.048 calculated on F for 3314 reflections with $I > 2.0\sigma(I)$, 0.112 calculated on F^2 for 4154 reflections with $I > -3.0\sigma(I)$ and 1.02 for 4154 reflections, respectively. The maximum and minimum peaks on the final difference Fourier map corresponded to 0.50 and -0.39 e[−]/Å³, respectively. All calculations were performed using the CrystalStructure³⁰ software package. The molecular structure is shown in Figure 2. Crystallographic data (excluding structure factors) have been deposited with the Cambridge Crystallographic Data Centre as supplementary publication number CCDC 215034. Copy of the data can be obtained, free of charge, on application to CCDC, 12 Union Road, Cambridge, CB1 1EZ, UK (fax: +44(0)-1223-3363033 or e-mail: deposit@ccdc.cam.ac.uk).

3.7. Feeding experiments

Three portions of the seed culture were transferred to 100 mL each of the production medium in 500 mL Erlenmeyer flasks which were grown shaking (200 rpm) at 28°C. Labelled sodium acetate in sterilised water was added (20 mg per 100 mL medium, total 1.8 L) to a 2-day culture followed by fermentation for further 3 days. The yields of purified labelled 5 were 6.0 mg (experiment a from sodium [2-¹³C]acetate administration), 4.6 mg (experiment b from sodium [1-¹³C]acetate administration), and 4.0 mg

(experiment c from sodium [2-¹³C,²H₃]acetate administration). Enrichment of ¹³C was evaluated based on the inverse gated decoupled ¹³C NMR spectra (the following carbons were used for the intensity normalization: C-16 for sodium [1-¹³C]acetate administration; C-3 for sodium [2-¹³C]acetate and sodium [2-¹³C, ²H₃]acetate administrations). Incorporation rates of the respective enriched positions (%): (a) C-2 (3.3), C-4 (4.5), C-6 (5.0), C-8 (3.4), C-10 (4.9), C-12 (3.6), C-14 (3.8), C-16 (4.6); (b) C-1 (2.4), C-3 (2.7), C-5 (2.6), C-7 (2.6), C-9 (2.1), C-11 (2.5), C-13 (2.1), C-15 (2.3); (c) C-2 (6.5), C-4 (8.6), C-6 (10.0), C-8 (7.2), C-10 (9.3), C-12 (9.3), C-14 (11.1), C-16 (9.6). ²H NMR spectrum of the sample from the experiment (c) indicated the relative deuterium intensity at C-16 to be 0.72 with C-8 (1.00) as a reference.

Acknowledgements

We thank Dr Motoo Shiro and Mr Toshiaki Hayashi, Rigaku Corporation, Japan for X-ray crystallographic analysis. We thank Professor Robert Thomas, Biotics Limited, for valuable discussion. This research was supported by grants from the Japan Society for the Promotion of Science (JSPS) and the Royal Society (JP-UK Bilateral Research Program to K. I., K. I. B., and G. R. S.) and BBSRC (Japan Partnering Award). T. T. was a recipient of JSPS Research Fellowship for Young Scientists (PD). We thank David A. Hopwood for critical reading of the manuscript.

References

- Bentley, S. D.; Chater, K. F.; Cerdeno-Tarraga, A. M.; Challis, G. L.; Thomson, N. R.; James, K. D.; Harris, D. E.; Quail, M. A.; Kieser, H.; Harper, D.; Bateman, A.; Brown, S.; Chandra, G.; Chen, C. W.; Collins, M.; Cronin, A.; Fraser, A.; Goble, A.; Hidalgo, J.; Hornsby, T.; Howarth, S.; Huang, C. H.; Kieser, T.; Larke, L.; Murphy, L.; Oliver, K.; O'Neil, S.; Rabinowitsch, E.; Rajandream, M. A.; Rutherford, K.; Rutter, S.; Seeger, K.; Saunders, D.; Sharp, S.; Squares, R.; Squares, S.; Taylor, K.; Warren, T.; Wietzorrek, A.; Woodward, J.; Barrell, B. G.; Parkhill, J.; Hopwood, D. A. *Nature* **2002**, *417*, 141–147.
- Hopwood, D. A. *Microbiology* **1999**, *145*, 2183–2202. Bibb, M. J. *Microbiology* **1996**, *142*, 1335–1344. Chater, K. F. *Microbiology* **1998**, *144*, 1465–1478.
- Zeeck, A.; Christiansen, P. *Liebigs Ann. Chem.* **1969**, *724*, 172–182.
- Hopwood, D. A. *Chem. Rev.* **1997**, *97*, 2465–2597.
- Ichinose, K.; Taguchi, T.; Ebizuka, Y.; Hopwood, D. A. *Acinomyetologica* **1998**, *12*, 99–109.
- Taguchi, T.; Ebizuka, Y.; Hopwood, D. A.; Ichinose, K. *J. Am. Chem. Soc.* **2001**, *123*, 11376–11380.
- Sciara, G.; Kendrew, S. G.; Miele, A. E.; Marsh, N. G.; Federici, L.; Malatesta, F.; Scimperia, G.; Savino, C.; Vallone, B. *EMBO J.* **2003**, *22*, 205–215.
- Ichinose, K.; Bedford, D. J.; Tornus, D.; Bechthold, A.; Bibb, M. J.; Revill, W. P.; Floss, H. G.; Hopwood, D. A. *Chem. Biol.* **1998**, *5*, 649–659.
- Ichinose, K.; Ozawa, M.; Itou, K.; Kunieda, K.; Ebizuka, Y. *Microbiology* **2003**, *149*, 1633–1645.

10. Gorst-Allman, C. P.; Rudd, B. A. M.; Chang, C.-j.; Floss, H. G. *J. Org. Chem.* **1981**, *46*, 455–456.
11. Fernández-Moreno, M. A.; Martínez, E.; Caballero, J. L.; Ichinose, K.; Hopwood, D. A.; Malpartida, F. *J. Biol. Chem.* **1994**, *269*, 24854–24863.
12. Ichinose, K.; Surti, C.; Taguchi, T.; Malpartida, F.; Booker-Milburn, K. I.; Stephenson, G. R.; Ebizuka, Y.; Hopwood, D. A. *Bioorg. Med. Chem. Lett.* **1999**, *9*, 395–400.
13. Taguchi, T.; Itou, K.; Ebizuka, Y.; Malpartida, F.; Hopwood, D. A.; Surti, C. M.; Booker-Milburn, K. I.; Stephenson, G. R.; Ichinose, K. *J. Antibiot.* **2000**, *53*, 144–152.
14. Cole, S. P.; Rudd, B. A. M.; Hopwood, D. A.; Chang, C.-J.; Floss, H. G. *J. Antibiot.* **1987**, *40*, 340–347.
15. The numbering given for discussion in the text is based on the biosynthetic origin.
16. Preliminary account for this paper was reported: Taguchi, T.; Ebizuka, Y.; Hopwood, D. A.; Ichinose, K. *Tetrahedron Lett.* **2000**, *41*, 5253–5256.
17. Harada, N.; Nakanishi, K. *Acc. Chem. Res.* **1972**, *5*, 257–263.
18. Bisang, C.; Long, P. F.; Cortes, J.; Westcott, J.; Crosby, J.; Matharu, A. L.; Cox, R. J.; Simpson, T. J.; Staunton, J.; Leadlay, P. F. *Nature* **1999**, *401*, 502–505.
19. Florova, G.; Kazanina, G.; Ryenolds, K. A. *Biochemistry* **2002**, *41*, 10462–10471.
20. Krupa, J.; Lessmann, H.; Lackner, H. *Liebigs Ann. Chem.* **1989**, *1989*, 699–701.
21. Bibb, M. J.; Sherman, D. H.; Omura, S.; Hopwood, D. A. *Gene* **1994**, *142*, 31–39.
22. Lombó, F.; Blanco, G.; Fernández, E.; Méndez, C.; Salas, J. A. *Gene* **1996**, *172*, 87–91.
23. Gerlitz, M.; Meurer, G.; Wendt-Pienkowski, M.; Madduri, K.; Hutchinson, C. R. *J. Am. Chem. Soc.* **1997**, *119*, 7392–7392.
24. Lomovskaya, N.; Otten, S. L.; Doi-Katayama, Y.; Fonstein, L.; Liu, X.-C.; Takatsu, T.; Inventi-Sokari, A.; Filippini, S.; Torti, F.; Colombo, A. L.; Hutchinson, C. R. *J. Bacteriol.* **1999**, *181*, 305–318.
25. Rajgarhia, V. B.; Strhol, W. R. *J. Bacteriol.* **1997**, *179*, 2690–2696.
26. Chater, K. F.; Bruton, C. J.; King, A. A.; Suarez, J. E. *Gene* **1982**, *19*, 21–32.
27. Kieser, T.; Bibb, M. J.; Buttner, M. J.; Chater, K. F.; Hopwood, D. A. *Practical Streptomyces Genetics*; John Innes Foundation: Norwich, 2000.
28. Sheldrick, G. M. *SHELXS-97: Program for the Solution of Crystal Structures*, University of Göttingen: Germany, 1997.
29. Watkin, D. J.; Prout, C. K.; Carruthers, J. R. *CRYSTALS Issue 10*; Chemical Crystallography Laboratory: Oxford, 1996.
30. Rigaku and Rigaku/MS. *CrystalStructure*. Crystal Structure Analysis Package; Rigaku, Tokyo, Japan and Rigaku/MS, Texas, USA, 2003.